Desalination and Water Treatment
www.deswater.com

doi: 10.5004/dwt.2021.26652

214 (2021) 114–119
February

Influence of hydrolysis, solvent and PVP addition on the porosity of PSF/PUR blend partly degradable hollow fiber membranes evaluated using the MeMoExplorer software

Wioleta Sikorska*, Małgorzata Przytulska, Monika Wasyłeczko, Cezary Wojciechowski, Juliusz L. Kulikowski, Andrzej Chwojnowski

Nałęcz Institute of Biocybernetics and Biomedical Engineering, Polish Academy of Sciences, Trojdena 4 Str., 02-109 Warsaw, Poland, emails: wsikorska@ibib.waw.pl (W. Sikorska), mprzytulska@ibib.waw.pl (M. Przytulska), mwasyleczko@ibib.waw.pl (M. Wasyłeczko), cwojciechowski@ibib.waw.pl (C. Wojciechowski), jkulikowski@ibib.waw.pl (J.L. Kulikowski), achwojnowski@ibib.waw.pl (A. Chwojnowski)

Received 17 March 2020; Accepted 28 May 2020

ABSTRACT

Asymmetric hollow fiber membranes were prepared by a dry/wet phase inversion process. Polysulfone and 2 types of polyurethanes (PUR) (with a different percentage share of ester bonds in PUR structure) were used as membrane-forming materials, N-methyl-2-pyrrolidone or N,N-dimethylformamide as a solvent and polyvinylpyrrolidone as a pore precursor addition. The membranes were treated with NaOH solution (hydrolysis process) due to the presence of ester bonds in the PUR structure. Scanning electron microscopy (SEM) was used to analyze the morphology of the membranes. The influence of hydrolysis process, the type of solvent and pore precursor addition on the porosity was studied. Differences of the porosity in various membranes were evaluated by the MeMoExploror software using SEM images.

Keywords: Porosity evaluation; Polysulfone-polyurethane blend hollow fiber membranes; Partly degradable membranes; MeMo Explore software

1. Introduction

The key factor in the development and application of membranes is the control of its morphology. Membrane pore size and membrane porosity tend to govern membrane morphology and impact membrane performance and membrane fouling. Porous membranes are very important and play a key role in different areas of biomedical application and technology. They are used for example as drug carrier systems, tissue engineering, medical implantable materials and biotechnology (chromatography, protein synthesis) [1–7]. It is known that the morphology of membranes can be changed by using different methods: heat treatment, plasma treatment, pore former or polymer additive, change of solvent or hydrolysis process [7–20].

A lot of various equipment, methods and computer software is used to study the porosity and pore size of membranes such as gravimetric method, mercury porosimetry, liquid displacement method, scanning electron microscopy (SEM) analysis, microcomputed tomography imaging, permeability-based method, capillary flow porometry, CAD models (for 3D scaffolds design) [6,21–26]. Wang et al. [27] presented a simple approach to determine pore size and porosity of hollow fiber membranes. This method was based on the resistance model and Poiseuille and Knudsen gas transport mechanisms.

The methods of computer-aided analysis of membrane pores elaborated in the Department of Biomaterials and Biotechnological Systems of the Nalecz Institute of Biocybernetics and Biomedical Engineering PAS were presented in several studies [28–30]. A novelty of the methods

* Corresponding author.

consists of fully automatic identification, contouring, size measuring and classification of the pores in SEM images of the specimens of the examined membranes. The above-mentioned operations are performed by a MeMoExplorer software system. The system was used, in particular, to estimate the porosity in polyvinylpyrrolidone (PVP) membranes [28], co-poly-L-lactide-glycolide/polyethersulfone membranes [29] and to show the changes in polysulfone (PSF)/polyurethanes (PUR) blend hollow fiber membranes after the hydrolysis process [30].

This study presents a computer-aided assessment of the porosity of membranes using the MeMoExplorer software. The PSF/PUR blend hollow fiber membranes were obtained by using different casting solutions (2 types of solvents and PURs, PVP addition) and treated with NaOH water solution (hydrolysis process). The SEM images of membranes before and after hydrolysis were analyzed using the MemoExplorer software and the influence of hydrolysis process, type of solvent and PVP addition on porosity was evaluated.

2. Experiments

2.1. Materials

PSF Udel 1700 NT LCD from Dow Corning (United States), M.W. 70 kD; polyurethanes with ester bonds in the structure (different % of ester bonds) (PUR) (synthesized independently using professor Rokicki's patent); N-methyl-2-pyrrolidone (NMP) from Fluka (Poland); N,N-dimethylformamide (DMF) from Chempur (Poland); PVP from Sigma-Aldrich (United States); sodium hydroxide (NaOH) from POCH; water 18,2 MΩ cm from MiliQ installation were used (United States).

2.2. Hollow fiber membranes preparation

The PSF and PUR were dissolved in NMP or DMF in two different flasks and stirred at 20°C temperature until complete dissolution. Received solutions were mixed in a flask for 24 h. The PSF:PUR weight ratio was constant: 8:2. A concentration of the polymers in NMP or DMF solution was 17% of the total solution's weight. The compositions of membranes casting solutions are presented in Table 1.

Eight types of membranes were obtained using a dry/wet-spinning, phase inversion technique through the extrusion of polymeric solution. The spinning process was conducted at room temperature. Obtained membranes (20 capillaries, 5.8 cm long) were put into propylenes modules.

Table 1
Compositions of the membranes casting solutions

Membrane	PUR	Solvent	PVP addition
PSF/PUR-2	PUR 9	NMP	–
PSF/PUR-5		DMF	
PSF/PUR-8	PUR 10	NMP	
PSF/PUR-11		DMF	
PSF/PUR-13	PUR 9	NMP	50% of PSF weight
PSF/PUR-14		DMF	
PSF/PUR-15	PUR 10	NMP	
PSF/PUR-16		DMF	

2.3. Hydrolysis process

The PSF/PUR membranes were treated with a 1 M NaOH solution using the flowing method. 1 dm^3 of NaOH solution was passed through the module passing inside the hollow fibers and flowing through the membrane's walls to the outside. The flowing time lasted from 1 to 3 d.

2.4. SEM analysis

SEM was used to characterize the morphology of obtained membranes. Hitachi TM-1000 microscope was used. Membranes were broken in liquid nitrogen and coated with a 10-nm gold layer using a sputtering device (EMITECH K 550X).

2.5. Evaluation of porosity using The MeMo Explorer software

The experiments were aimed at the evaluation of:

- the influence of hydrolysis on the porosity in various types of membranes;
- the influence of different solvents on the porosity in various types of membranes;
- the influence of pore precursor addition on the porosity in various types of membranes;
- parameter stability (characterized by the ratio: standard deviation of the porosity coefficient/averaged value of the porosity coefficient) in the series of samples drawn from the membranes.

In the experiments 8 types of membranes before hydrolysis (denoted by #2, #5, #8, #11, #13, #14, #15, #16) and 8 types after hydrolysis (denoted by #2h, #5h, #8h, #11h, #13h, #14h, #15h, #16h) were taken into consideration. The number of SEM images of membrane sections for technical reasons was not constant and varied from 15 up to 30 images per type of membrane. In each image, several sections (regions of interest) were selected for image analysis. The first steps of image analysis, performed by using the MeMoExplorer software, consisted in:

- the selection and contouring of pores;
- the measurement of their surfaces;
- the partition of pores into 8 size-classes (<3, 3–8, 8–20, 20–80, 80–100, 100–150, 150–300, >300 μm)
- the measurement of total areas covered by pores of given classes: $s^0_{i,j,k}$ – before hydrolysis, $s^H_{i,j,k}$ – after hydrolysis, where i is the index of the membrane, j is the index of the size-class of pores, k is the index of the image-segment under examination.
- the calculation of basic statistical parameters:
  - mean values of areas in given classes of membranes (i) obtained by using given technologies (0, H), covered by pores of given size-classes (j):

$$S^0_{i,j} = \text{Mean}_{(k)}\left(s^0_{i,j,k}\right) \tag{1a}$$

$$S_{i,j}^{H} = \text{Mean}_{(k)}\left(s_{i,j,k}^{H}\right) \quad (1b)$$

- standard deviations of the above-mentioned variables:

$$\Delta_{i,j}^{0} = \text{Std}_{(k)}\left(s_{i,j,k}^{0}\right) \quad (2a)$$

$$\Delta_{i,j}^{H} = \text{Std}_{(k)}\left(s_{i,j,k}^{H}\right) \quad (2b)$$

3. Results

On the basis of the above-described parameters several summarizing statistics were evaluated. The data have been divided by the area S of image segments (fixed in all images analyzed by the MeMoExplorer system) in order to be presented as dimensionless porosity coefficients κ.

3.1. Influence of the hydrolysis process

For the influence of the hydrolysis process on the porosity of membranes assessment the values $S_{i,j}^{0}$ and $S_{i,j}^{H}$ have been measured. In Fig. 1 several examples of sections of membranes before and after hydrolysis are shown. The differences in fine morphological structure in the pairs of the corresponding types of membranes are remarkable.

The calculated values $S_{i,j}^{0}$ and $S_{i,j}^{H}$ (marked as Mean) are presented in pairs in Fig. 2. Moreover, the corresponding standard deviations (Std) to them have been added. This enables a direct comparison of the porosity coefficients in various types of membranes before and after hydrolysis, as well as the evaluation of the accuracy of the comparisons.

An increase in the porosity coefficients occurred in all pairs of membranes except for the (#5^0, #5^H) one. In all cases, the differences are varying within the intervals outlined by the standard deviations, the last being large because of a low number of segments (regions of interest) available in individual samples. Nevertheless, the effect of $S_{i,j}^{H}$ exceeding $S_{i,j}^{0}$ in the examined pairs of specimens remains statistically stable. Similarly, the variations of the mean values of the porosity coefficient in the series of membranes are gathered around their averaged values and kept within the intervals fixed by the averaged standard deviations. This leads to the conclusion that the proposed membranes (before, as well as after hydrolysis) are practically characterized by satisfactory stability of porosity.

3.2. Solvent influence

For the evaluation of solvent influence on the porosity coefficient of membranes the following pairs of membranes were examined: (#2^0, #5^0), (#8^0, #11^0), (#13^0, #14^0), (#15^0, #16^0). The results in Fig. 3 are presented in triplets indicating mean porosity coefficients in pairs of membranes obtained with different solvents, as well as differences between them. Standard deviations as an extension of the corresponding mean values are presented as well. The small positive effect of using NMP as a solvent can be observed only in the pair (#2^0, #5^0), and the effect of using DMF as a solvent can be observed in pairs: (#8^0, #11^0), (#13^0, #14^0) and (#15^0, #16^0).

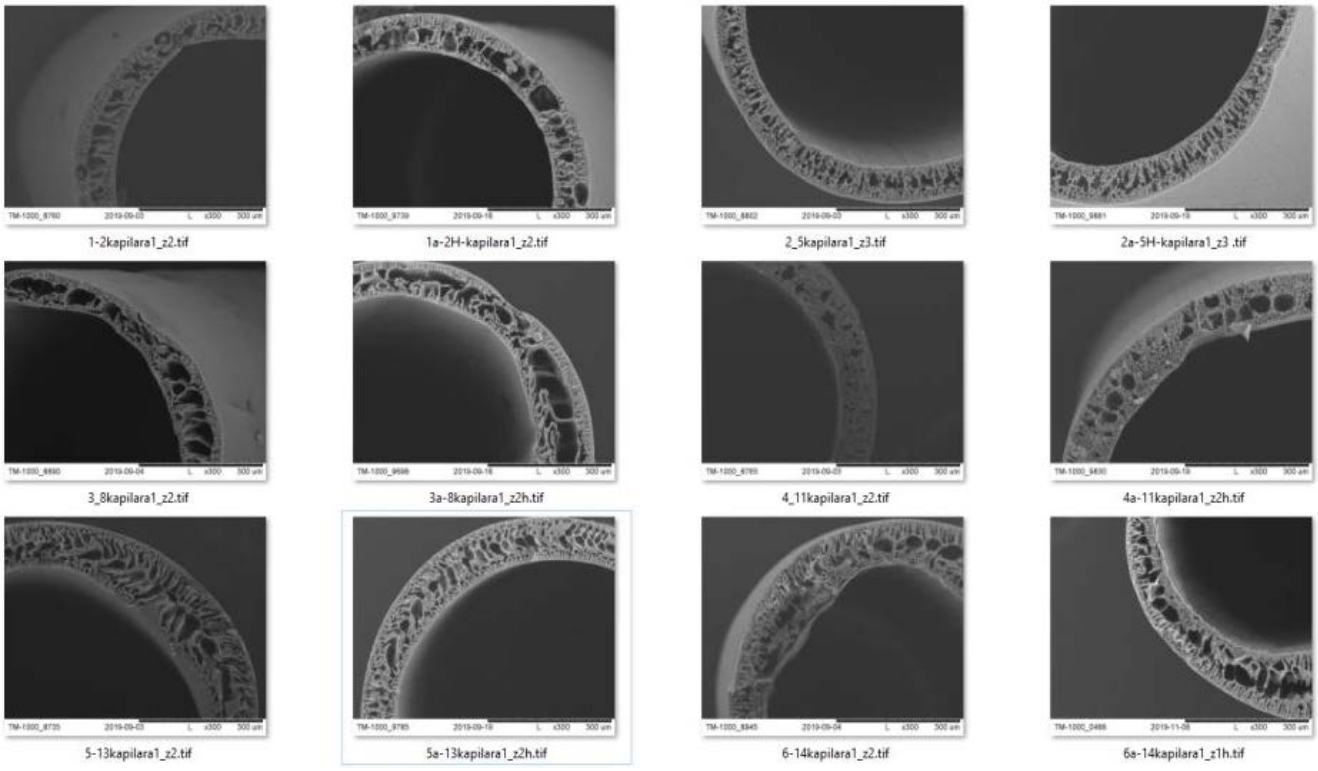

Fig. 1. Pairs of membranes before and after hydrolysis.

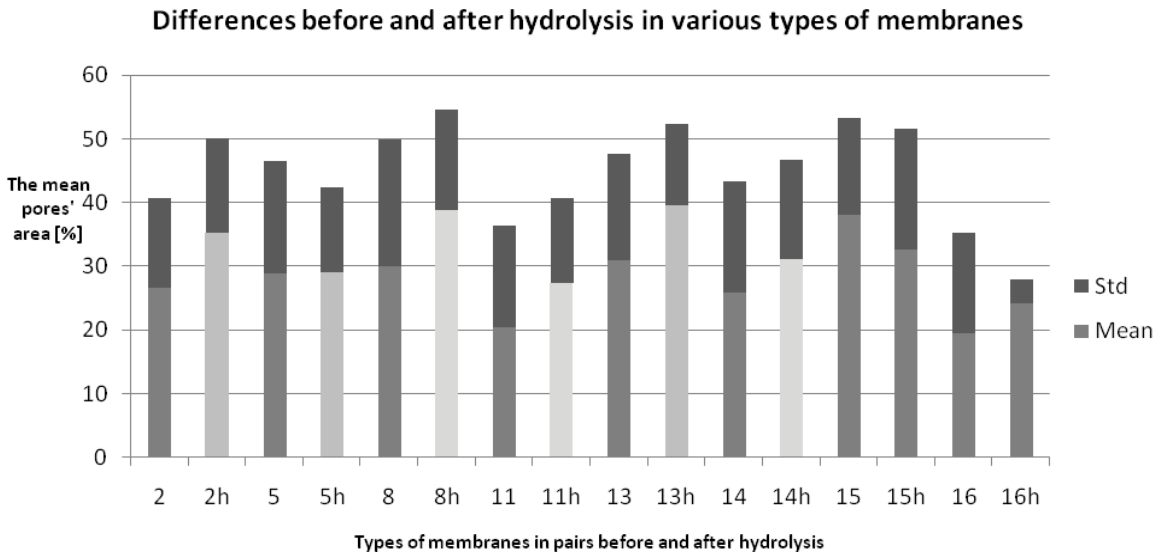

Fig. 2. The influence of hydrolysis on the porosity coefficient in various types of membranes.

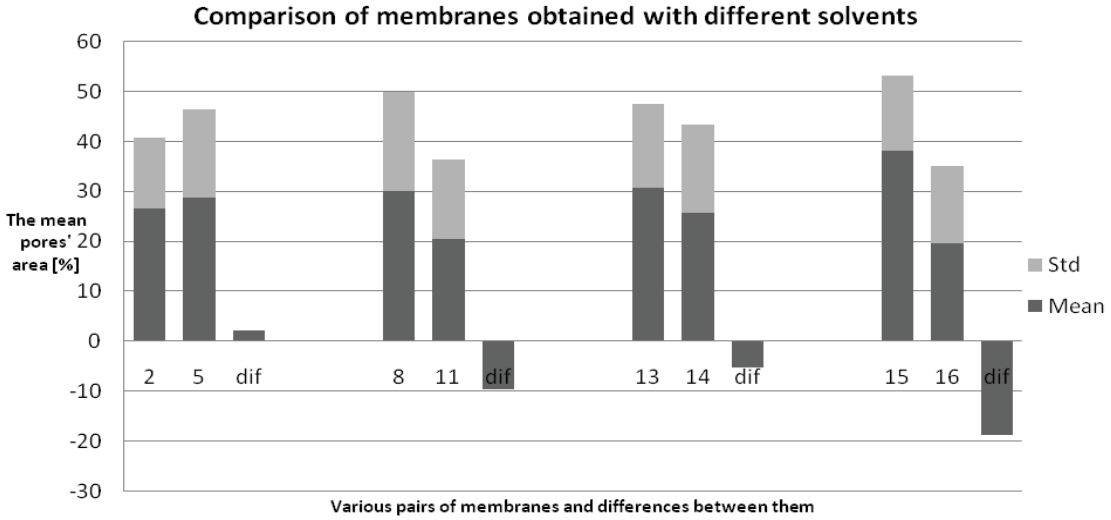

Fig. 3. The influence of using solvents on the porosity coefficient in selected types of membranes.

3.3. Influence of pore precursor addition

The influence of pore precursor addition on the porosity coefficient was examined for the following pairs of membranes (#2^0, #13^0), (#5^0, #14^0), (#8^0, #15^0), (#11^0, #16^0). The results are shown in Fig. 4. Once again, they are presented by four triplets indicating the mean porosity coefficient, extended by the corresponding standard deviations, without or with the addition of pore precursor (PVP). The third element of the triplet presents the difference between the mean values. It can be noted that the positive effect of using pore precursor in the pairs (#2^0, #13^0) and (#8^0, #15^0) took a significant value.

3.4. Instability coefficients for different types of membranes

The instability of membrane parameters in the series of samples can be characterized by the ratio: standard deviation of the porosity coefficient/averaged value of the porosity coefficient calculated in the set of images of a given type (*i*) of a membrane. Taking into account that the porosity coefficients κ have been calculated for a fixed image area *S* and the contributions of the pores of different size-classes (*j*) are statistically independent, the unstability coefficients could be given directly by the ratios Δ_i^0/S_i^0 or Δ_i^H/S_i^H, where:

$$S_i^0 = \sum_{(j)} \left(S_{i,j}^0 \right) \tag{3a}$$

$$S_i^H = \sum_{(j)} \left(S_{i,j}^H \right) \tag{3b}$$

and

$$\Delta_i^0 = \Gamma_{(j)} \left(\Delta_{i,j}^0 \right) \tag{4a}$$

$$\Delta_i^H = \Gamma_{(j)}\left(\Delta_{i,j}^H\right) \tag{4b}$$

where $\Gamma_{(j)}$ denotes a geometrical mean (a square-root of the sum of squared components).

However, the comparison of so-defined instability coefficients in different membranes leads to false results because the values Δ_i^0 and Δ_i^H strongly depend not only on the real instability of membrane parameters but also on the number of samples used for their evaluation. Roughly speaking, the standard deviations decrease with the square-root of the number K_i of samples taken into consideration. Therefore, the above-mentioned instability coefficients for their comparability should be normalized according to the formulae:

$$\kappa_i^0 = \sqrt{K_i} \cdot \frac{\Delta_i^0}{S_i^0} \tag{5a}$$

$$\kappa_i^H = \sqrt{K_i} \cdot \frac{\Delta_i^H}{S_i^H} \tag{5b}$$

The results are presented in Fig. 5. The doublets show the normalized unstability coefficients before and after hydrolysis in 8 types of membranes. The membrane #16^H occurred the best one from the stability (minimal unstability coefficient) point of view. A stabilizing effect of hydrolysis (lower levels of normalized unstability coefficient in the case of hydrolysis) in all types of membranes is remarkable.

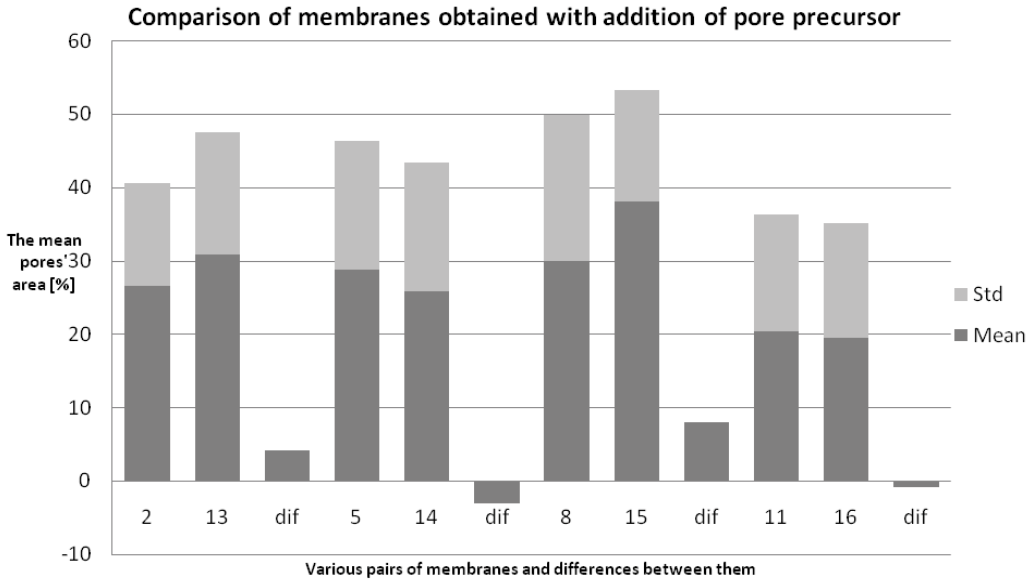

Fig. 4. The influence of pore precursor addition on the porosity coefficient in selected types of membranes.

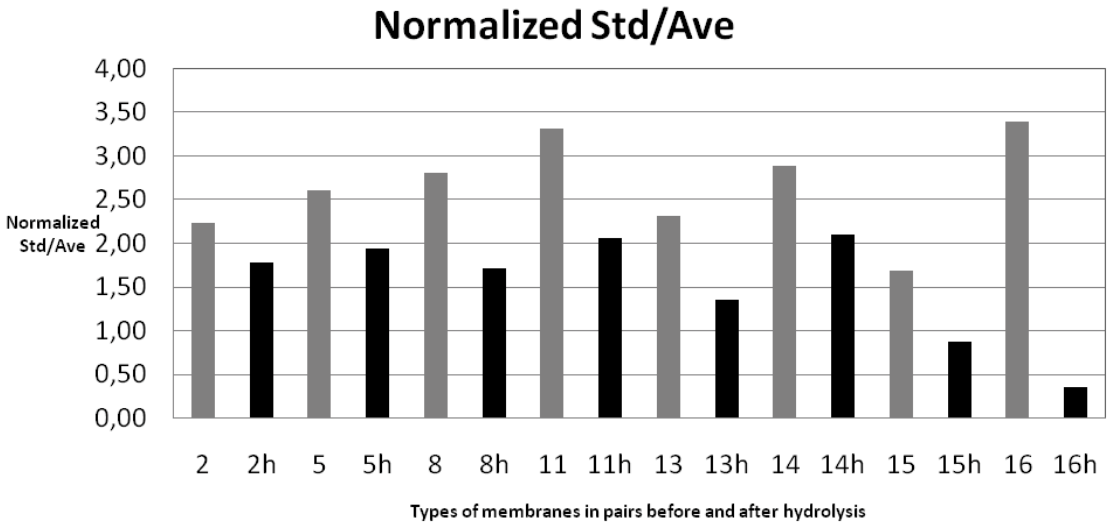

Fig. 5. Instability coefficients for different types of membranes.

4. Conclusions

The aim of this work was the examination of the influence of the hydrolysis process, the type of solvent and pore precursor addition to the casting solution on the final porosity of membranes. A positive effect of hydrolysis on a statistically significant level of the porosity coefficient increasing was observed. This leads to the conclusion that hydrolysis has an impact on PUR degradation. A spatial evenness of the porosity coefficient in individual specimens and its stability in the series of specimens of the examined membranes on a statistically significant level was observed. The positive effect of using DMF as a solvent in three (out of four) pairs of membranes have been observed. Positive effects of using pore precursor in two (out of four) pairs of examined membranes have been observed. It can be concluded that: (1) the hydrolysis process leads to partial degradation of PUR in the membrane structure and causes the increase in porosity; (2) the type of solvent has an impact on the porosity of the PSF/PUR blend hollow fiber membranes.

References

[1] H.-P. Hentze, M. Antonietti, Porous polymers and resins for biotechnological and biomedical applications, Rev. Mol. Biotechnol., 90 (2002) 27–53.

[2] R. Yakimova, R.M. Petoral Jr., G.R. Yazdi, C. Vahlberg, A. Lloyd Spetz, K. Uvdal, Surface functionalization and biomedical applications based on SiC, J. Phys. D: Appl. Phys., 40 (2007) 6435–6442.

[3] A.J. Rosenbloom, D.M. Sipe, Y. Shishkin, Y. Ke, R.P. Devaty, W.J. Choyke, Nanoporous SiC: a candidate semi-permeable material for biomedical applications, Biomed. Microdevices, 6 (2004) 261–267.

[4] D.H. Liang, B.S. Hsiao, B. Chu, Functional electrospun nanofibrous scaffolds for biomedical applications, Adv. Drug Delivery Rev., 59 (2007) 1392–1412.

[5] H.R. Oxley, P.H. Corkhill, J.H. Fitton, B.J. Tighe, Macroporous hydrogels for biomedical applications: methodology and morphology, Biomaterials, 14 (1993) 1064–1072.

[6] Q.L. Loh, C. Choong, Three-dimensional scaffolds for tissue engineering applications: role of porosity and pore size, Tissue Eng. Part B, 19 (2013) 485–502.

[7] A. Abdelrasoul, H. Doan, A. Lohi, C.-H. Cheng, Morphology control of polysulfone membranes in filtration processes: a critical review, ChemBioEng Rev., 2 (2015) 22–43.

[8] M. Kwong, A. Abdelrasoul, H. Doan, Controlling polysulfone (PSF) fiber diameter and membrane morphology for an enhanced ultrafiltration performance using heat treatment, Results Mater., 2 (2019) 100021.

[9] L. Zhang, L.-g. Liu, F.-l. Pan, D.-f. Wang, Z.-j. Pan, Effects of heat treatment on the morphology and performance of PSU electrospun nanofibrous membrane, J. Eng. Fibers Fabr., 7 (2012) 7–16.

[10] K.S. Kim, K.H. Lee, K. Cho, C.E. Park, Surface modification of polysulfone ultrafiltration membrane by oxygen plasma treatment, J. Membr. Sci., 199 (2002) 135–145.

[11] M.L. Steen, L. Hymas, E.D. Havey, N.E. Capps, D.G. Castner, E.R. Fisher, Low temperature plasma treatment of asymmetric polysulfone membranes for permanent hydrophilic surface modification, J. Membr. Sci., 188 (2001) 97–114.

[12] Y. Feng, K. Wang, J.F. Yao, P.A. Webley, S. Smart, H. Wang, Effect of the addition of polyvinylpyrrolidone as a pore-former on microstructure and mechanical strength of porous alumina ceramics, Ceram. Int., 39 (2013) 7551–7556.

[13] H. Matsuyama, T. Maki, M. Teramoto, K. Kobayashi, Effect of PVP additive on porous polysulfone membrane formation by immersion precipitation method, Sep. Sci. Technol., 38 (2003) 3449–3458.

[14] B. Chakrabarty, A.K. Ghoshal, M.K. Purkait, Preparation, characterization and performance studies of polysulfone membranes using PVP as an additive, J. Membr. Sci., 315 (2008) 36–47.

[15] M.-J. Han, S.-T. Nam, Thermodynamic and rheological variation in polysulfone solution by PVP and its effect in the preparation of phase inversion membrane, J. Membr. Sci., 202 (2002) 55–61.

[16] B. Chakrabarty, A.K. Ghoshal, M.K. Purkait, Effect of molecular weight of PEG on membrane morphology and transport properties, J. Membr. Sci., 309 (2008) 209–221.

[17] G. Arthanareeswaran, D. Mohan, M. Raajenthiren, Preparation, characterization and performance studies of ultrafiltration membranes with polymeric additive, J. Membr. Sci., 350 (2010) 130–138.

[18] S.S. Madaeni, A. Rahimpour, Effect of type of solvent and non-solvents on morphology and performance of polysulfone and polyethersulfone ultrafiltration membranes for milk concentration, Polym. Adv. Technol., 16 (2005) 717–724.

[19] C. Wojciechowski, A. Chwojnowski, L. Granicka, E. Łukowska, Polysulfone/cellulose acetate blend semi degradable capillary membranes preparation and characterization, Desal. Water Treat., 64 (2017) 365–371.

[20] C. Wojciechowski, A. Chwojnowski, L. Granicka, E. Łukowska, M. Grzeczkowicz, Polysulfone/polyurethane blend degradable hollow fiber membranes preparation and transport–separation properties evaluation, Desal. Water Treat., 57 (2016) 22191–22199.

[21] L. Ghasemi-Mobarakeh, D. Semnani, M. Morshed, A novel method for porosity measurement of various surface layers of nanofibers mat using image analysis for tissue engineering applications, J. Appl. Polym. Sci., 106 (2007) 2536–2542.

[22] Q.P. Pham, U. Sharma, A.G. Mikos, Electrospun poly (ε-caprolactone) microfiber and multilayer nanofiber/microfiber scaffolds: characterization of scaffolds and measurement of cellular infiltration, Biomacromolecules, 7 (2006) 2796–2805.

[23] Y. Zhang, M.Q. Zhang, Synthesis and characterization of macroporous chitosan/calcium phosphate composite scaffolds for tissue engineering, J. Biomed. Mater. Res., 55 (2001) 304–312.

[24] A.R. El-Ghannam, Advanced bioceramic composite for bone tissue engineering: design principles and structure-bioactivity relationship, J. Biomed. Mater. Res. Part A, 69 (2004) 490–501.

[25] S.T. Ho, D.W. Hutmacher, A comparison of micro CT with other techniques used in the characterization of scaffolds, Biomaterials, 27 (2006) 1362–1376.

[26] W. Sun, B. Starly, A. Darling, C. Gomez, Computer-aided tissue engineering: application to biomimetic modelling and design of tissue scaffolds, Biotechnol. Appl. Biochem., 39 (2004) 49.

[27] R. Wang, T.-S. Chung, Determination of pore sizes and surface porosity and the effect of shear stress within a spinneret on asymmetric hollow fiber membranes, J. Membr. Sci., 188 (2001) 29–37.

[28] M. Przytulska, A. Kruk, J.L. Kulikowski, C. Wojciechowski, A. Gadomska-Gajadhur, A. Chwojnowski, Comparative assessment of polyvinylpyrrolidone type of membranes based on porosity analysis, Desal. Water Treat., 75 (2017) 18–25.

[29] M. Przytulska, J.L. Kulikowski, M. Wasyłeczko, A. Chwojnowski, D. Piętka, The evaluation of 3D morphological structure of porous membranes based on a computer-aided analysis of their 2D images, Desal. Water Treat., 128 (2018) 11–19.

[30] W. Sikorska, C. Wojciechowski, M. Przytulska, G. Rokicki, M. Wasyłeczko, J.L. Kulikowski, A. Chwojnowski, Polysulfone–polyurethane (PSF-PUR) blend partly degradable hollow fiber membranes: preparation, characterization, and computer image analysis, Desal. Water Treat., 128 (2018) 383–391.